Toroidal ion-pressure-gradient-driven drift instabilities and transport revisited

Cite as: Physics of Fluids B: Plasma Physics 1, 109 (1989); https://doi.org/10.1063/1.859206
Submitted: 14 March 1988 . Accepted: 06 September 1988 . Published Online: 04 June 1998

H. Biglari, P. H. Diamond, and M. N. Rosenbluth

Toroidal ion-pressure-gradient-driven drift instabilities and transport revisited

H. Biglari, P. H. Diamond, and M. N. Rosenbluth
Department of Physics B-019, University of California at San Diego, La Jolla, California 92093 and General Atomics, San Diego, California 92138

(Received 14 March 1988; accepted 6 September 1988)

A unified theory of ion-pressure-gradient-driven drift wave instabilities and transport is presented, which ties the long-wavelength trapped-ion mode to the moderate-wavelength hydrodynamic mode in toroidal geometry. An analytic dispersion relation that retains ion drift resonances, and keeps the leading-order contribution from finite Larmor radius effects and parallel compressibility, is derived. Results indicate that the slab and toroidal branches of these instabilities are of comparable importance, and are both strong candidates to explain the observed anomalous ion loss in toroidal fusion devices. However, it is concluded that in the limit of flat-density profiles characteristic of H-mode discharges, the stabilizing influence of perpendicular compressibility is insufficient to corroborate an improvement, if any, in *ion* confinement quality. Mixing-length expressions for the fluctuation amplitudes and both electron and ion transport coefficients are derived. Results also indicate that the heretofore experimentally observed favorable current scaling of the energy confinement time may saturate in low ion-collisionality discharges. Finally, it is shown that a population of energetic trapped particles, such as those that may be produced during radio frequency or perpendicular neutral beam heating, can significantly exacerbate the instability. Several suggestions for experiments are made to help in differentiating among various anomalous transport scenarios.

I. INTRODUCTION

Evidence that instabilities and turbulence driven by the ion-pressure gradient can dramatically degrade the quality of ion thermal confinement has been borne out to an impressive degree by a number of recent experiments. The first clear indication of anomalous ion loss came in connection with the D-III experiment,[1] where the Ohmic confinement time was observed to saturate at high density ($\tau_E \propto n$) almost an order of magnitude below the predictions of neoclassical theory.[2,3] Experiments on all subsequent tokamaks have reconfirmed this observation.[4–6] Further insight into the nature of the problem came with the observation on Alcator-C[4] that the injection of frozen pellets of deuterium into the ambient plasma acted to reduce the level of ion thermal conduction losses to their neoclassical value, while leaving the anomaly in the electron thermal losses unchanged. The improvement of ion energy confinement with pellet injection received further corroboration in recent experiments performed on both the TFTR[7] and ASDEX[8] tokamaks. Perhaps the most dramatic evidence in favor of the association between anomalous ion losses and the premature saturation of energy confinement time with density came in connection with recent heterodyne far-infrared (FIR) laser scattering experiments on TEXT.[9] By examining the spectral characteristics of electrostatic fluctuations at various densities, Brower and co-workers observed the onset of fluctuations propagating in the ion direction to coincide with the saturation of τ_E with density. That the quality of ion confinement degrades further in the L-mode regime of auxiliary heating, has also been evidenced in the D-III tokamak.[4] In that experiment, inferences of the ion thermal diffusivity (χ_i) based on ion temperature profile measurements indicate that in the bulk of the plasma ($0.2 \lesssim r/a \lesssim 0.8$, where a is the minor radius), χ_i is not only larger in magnitude, but also exhibits a radial profile significantly at odds with the predictions of neoclassical theory. Finally, the recent observation on ASDEX[10] of a regime of improved confinement with *counter* neutral beam injection, which results in an inward particle pinch and consequent steepened density profiles, is again consistent with the results of pellet injection experiments mentioned earlier. The results of all these experiments has lent strong credence to the theory that losses stemming from ion-pressure-gradient-driven drift waves are responsible for the premature saturation of the energy confinement time.

As originally formulated in slab geometry,[11–15] this so-called sonic or slablike η_i mode ($\eta_i = d \ln T_i / d \ln n_i$, where T_i and n_i are, respectively, the ion temperature and density) evolves when unstable ion acoustic waves couple to radial ion pressure gradients. As was noted by Horton *et al.*[16] and Guzdar *et al.*,[17] the introduction of toroidal curvature completely changes the nature of the mode. In toroidal geometry, the mode has more of a ballooning structure and is driven by unfavorable magnetic curvature rather than acoustic waves. In low plasma collisionality regimes, ion trapping enters as a new and important added ingredient to this picture. These trapped-ion modes are not susceptible to parallel compression, and hence constitute the long-wavelength branch of the toroidal ion-pressure-gradient-driven family of instabilities.[18–20] In recent work, we have investigated the nonlinear evolution of the resonantly destabilized trapped-ion-temperature-gradient-driven instability.[21,22] Threshold-dependent, non-steady-state turbulence was shown to develop, leading to large levels of anomalous thermal and particle transport that, in turn, reconfigure the equilibrium tempera-

 0899-8221/89/010109-10$01.90

ture and density profiles in such a way as to return the system toward its marginal point. The main motivation for the present work is to tie the trapped-ion branch in with the well-known fluidlike toroidal ∇p_i-driven mode, and thus present a unified theory of ion-pressure-gradient-driven drift instabilities over all wavelengths.

It is reasonable to ask for experimental features sufficiently universal that any theoretically based transport scenario must be able to account for them. Three such requirements come to mind. The first is the universally observed improvement in confinement quality with increasing plasma current. Unfortunately, experimental evidence in favor of or against an *intrinsically local* current dependence is inconclusive at the time of this writing. Preliminary evidence from power balance calculations on the Joint European Torus (JET)[23] appears to imply a current scaling in the bulk heat flux.[24] Should this observation persist for the ion channel separately (there were no ion temperature profile measurements available on JET), the imperative will be for an intrinsic current dependence rather than one which is dynamically coupled to transport processes at the plasma edge. However, neither one nor the other can be dismissed at this time. A second requirement, which theories of ion-pressure-gradient-driven drift wave instabilities and transport must be able to account for, is the degradation in confinement with input power, which manifests itself indirectly in the Ohmic regime through the current dependence of the Ohmic input power, and directly in the L-mode regime of confinement when auxiliary sources of heating are utilized. Finally, an adequate theory must be able to simultaneously explain the improvement in confinement after the transition from L- to H-mode operation,[25–27] as well as that after pellet injection.[4,7] On first glance, these two requirements appear to be mutually incompatible, as the density profiles characteristic of H-mode discharges, in contrast to pellet-fueled plasmas, are very flat, and consequently force η_i to significantly exceed its threshold value. However, in the limit of very weak density gradients (i.e., $\eta_i \to \infty$), it has been shown by Tang *et al.*[28] that the relevant stability parameter governing these modes becomes L_{Ti}/R rather than $\eta_i = L_n/L_{Ti}$ (where $L_f^{-1} = -d\ln f/dr$). Moreover, Dominguez and Waltz[29] have suggested, based on a fluid analysis, that perpendicular compression can completely stabilize the instability. However, as we shall show here, fluid theory may not be optimal to uncover any stabilizing trends resulting from compressibility, and any threshold criteria so obtained can only be regarded as indicative.

Before presenting the details of the analysis, we provide here a preamble of what is to follow. As we pointed out in the preceding paragraph, a proper evaluation of the influence of perpendicular compression must have its foundation in kinetic theory. In Sec. II, we therefore begin by analytically deriving the dispersion relation for these instabilities from the gyrokinetic equation. The derivation fully retains magnetic drift resonances, and includes leading-order corrections resulting from finite ion Larmor radius (FLR) and parallel compressibility. After a general discussion of stability properties using Nyquist diagrammatic techniques, we make several analytically tractable approximations in order to elucidate the essence of the mode. Having accomplished our goal in uncovering the influence of perpendicular compression, we find it more feasible to continue our discussion of transport scaling within the context of fluid theory. In Sec. II C, we derive scaling laws for the thermal flux and diffusivity that have differences with those derived in the past.[16,28,30] The reasons for these differences are discussed. Ion-pressure-gradient-driven turbulence not only provides a direct loss mechanism for the ion channel, but can also degrade the quality of electron confinement. Noting that the dissipative trapped-electron mode is thought to be responsible for the degradation of the electron channel in the bulk of the plasma, we provide estimates of the level of particle and electron thermal transport that can be expected to ensue in response to ion turbulence. In Sec. III, we discuss the long-wavelength branch of these modes, namely trapped-ion-pressure-gradient-driven modes. It is shown that because of their longer wavelengths, thermal diffusion driven by the latter can significantly exceed the corresponding one for the hydrodynamic branch. In Sec. IV, we focus on the flat-density limit of these instabilities. When proper account is made for perpendicular compressibility, it is shown that, within the limits of the theory, the stability threshold associated with L_{Ti}/R is too stringent to ever be satisfied, making complete stabilization with respect to these modes unattainable. In Sec. V, we consider the interaction of an energetic trapped-particle species, such as those that are created during auxiliary heating, with the background plasma, and consider how the instabilities are affected. It is found that for a sufficiently localized energetic particle deposition profile, the instability can be exacerbated by unfavorably trapped energetic particles. We conclude the paper with a summary of the major results, and a discussion on how these results impact on experiments.

II. TOROIDAL ∇p_i-DRIVEN MODE

In order to have confidence in uncovering the influence of perpendicular compression, a kinetic theory must be employed in lieu of fluid theory. In this section, we derive the dispersion relation governing ∇p_i- driven modes using kinetic theory, and make analytically tractable approximations in order to capture the essential features of the mode. The relevant frequency ordering is given by

$$\omega_{be},\omega_{te} \gg \omega_{*i} > |\omega| \sim \omega_{di} > \omega_{bi},\omega_{ti},$$

where $\omega_b(\omega_t) = \oint dl/v_\parallel$ is the magnetic bounce (transit) frequency, $\omega_* = v_t^2 \hat{\mathbf{e}}_\parallel \cdot \nabla \ln n \times \mathbf{k}_\perp / 2\Omega_c = -k_\theta \rho v_t/2L_n$ is the diamagnetic drift frequency, $\omega_*^T = \eta\omega_*$, $\hat{\mathbf{e}}_\parallel = \mathbf{B}/B$ is the unit vector in the direction of the ambient, magnetic field, $\rho = v_t/\Omega_c$ is the Larmor radius, $v_t = (2T/m)^{1/2}$ is the thermal speed, $\Omega_c = eB/mc$ is the cyclotron frequency, $L_n = -(d\ln n/dr)^{-1}$ is the density gradient scale length, $k_\theta = m/r$ is the poloidal wave vector, $\omega_*' = \omega_* \times [1 + \eta(E/T - 3/2)]$, ω is the mode frequency, and $\omega_d = \mathbf{k}_\perp \cdot \mathbf{v}_d \simeq (\mu \nabla B + v_\parallel^2)\mathbf{e}_\parallel$; $\boldsymbol{\kappa} \times \mathbf{k}_\perp/\Omega_c = \tilde{\omega}_d(\bar{v}_\parallel^2 + \bar{v}_\perp^2/2) \times G(\hat{s},\mathbf{r})$ is the magnetic drift frequency, $\omega_d = -k_\theta \rho v_t/R$, $E = v^2/2$ is the energy per unit mass, $\bar{v} = v/v_t$, $\boldsymbol{\kappa} = \hat{\mathbf{e}}_\parallel \cdot \nabla \hat{\mathbf{e}}_\parallel$ is the magnetic curvature, and $G(\hat{s},\mathbf{r})$ contains the spatial

variation of ω_d. Ion trapping can thus be ignored, and the electron response is assumed to be adiabatic. The latter assumption is justified because electron dynamics plays essentially no role in the linear stability analysis; the same argument carries over to the case of the trapped-ion mode. Finally, it may be verified *a posteriori* that the right-hand side inequality bounds poloidal wavelengths from exceeding a banana width $\rho_b \simeq \epsilon^{-1/2} q \rho_i$. The perturbed circulating-ion response can be obtained from the gyrokinetic equation

$$\delta f_i = -(e\delta\phi/T_i)F_{Mi} + \delta h_{ic} \exp(-iL), \tag{1}$$

$$\delta h_{ic} = \frac{e\delta\phi}{T_i} J_0\left(\frac{k_\perp v_\perp}{\Omega_{ci}}\right) \frac{\omega - \omega^t_{*i}}{\omega - \omega_{di} - k_\parallel v_\parallel} F_{Mi},$$

$$\simeq \frac{e\delta\phi}{T_i}\left(1 - b_\perp \bar{v}_\perp^2 + \frac{(\omega_{ti}/\tilde{\omega}_{di})^2 \bar{v}_\parallel^2}{[\Omega - (\bar{v}_\parallel^2 + \bar{v}_\perp^2/2)]^2}\right) \times \frac{\Omega - \Omega^T_{*i}(\bar{v}_\parallel^2 + \bar{v}_\perp^2 + \eta_i^{-1} - \frac{3}{2})}{\Omega - (\bar{v}_\parallel^2 + \bar{v}_\perp^2/2)} F_{Mi}. \tag{2}$$

In the above, $\omega_{ti} = k_\parallel v_{ti}$ is the ion transit frequency, $L = \mathbf{e}_\parallel \cdot \mathbf{v}_\perp \times \mathbf{k}_\perp / \Omega_{ci}$ is the Larmor factor, J_0 is the zeroth-order Bessel function, $F_{Mi} = (n_0/\pi^{3/2} v_{ti}^3)\exp(-\bar{v}^2)$ is the unperturbed Maxwellian ion distribution function, δh_{ic} is the nonadiabatic circulating-ion response $\Omega = \omega/\tilde{\omega}_{di}$, $\Omega^T_{*i} = \omega^T_{*i}/\tilde{\omega}_{di} = R/2L_{Ti}$, and $b_\perp = (k_\perp \rho_i)^2/2$. We have made a small Larmor radius expansion, and in expanding the denominator in the first line of Eq. (2), we have taken note of the fact that odd $v_\parallel$ moments vanish. After some tedious manipulations, which are relegated to the Appendix, an analytic dispersion relation which retains drift resonance effects is derived:

$$D(\Omega) = D_0(\Omega) + D_{\rm FLR}(\Omega) + D_S(\Omega), \tag{3}$$

where

$$D_0(\Omega) = -(1+\tau^{-1}) + Y^2 + \Omega^T_{*i}\{[(1-\eta_i^{-1})/\Omega - 2]\, Y^2 + 2Y\},$$

$$\frac{D_{\rm FLR}}{b_\perp} = -Y^2 - 2\Omega(Y-1)^2 + \Omega^T_{*i}\left(2(\eta_i^{-1} + 2\Omega)(Y-1)^2 + \frac{Y^2}{\Omega\eta_i}\right),$$

$$\frac{D_S(\Omega)}{(\omega_{ti}/\tilde{\omega}_{di})^2} = \left[\Omega^T_{*i}\left(\eta_i^{-1} - \frac{3}{2}\right) - \Omega\right] \times \left[1 - \left(1 + \frac{1}{2\Omega}\right) Y + \frac{Y^2}{\Omega}\right] + \Omega^T_{*i}\left[\Omega - \left(\Omega + \frac{3}{2}\right) Y + \left(2 - \frac{1}{2\Omega}\right) Y^2\right],$$

and

$$Y = \Omega^{1/2} \exp(-\Omega) \int_{-\infty}^{\Omega} dz\, z^{-1/2} \exp z.$$

Some general results can be ascertained by performing a Nyquist analysis of Eq. (3). Thus one maps the upper complex frequency domain into the complex-D plane, and an instability criterion follows from the condition that the origin be encircled by the image contour. First note that

$$\Omega \to \pm\infty \Rightarrow D(\pm\infty) \sim -\tau^{-1} - b_\perp + \{1 - \Omega^T_{*i}[\eta_i^{-1} - b_\perp(\eta_i^{-1} - 1)]\}/\Omega,$$

$$\Omega = 0^+ \Rightarrow D(0^+) \simeq -(1+\tau^{-1}) + \pi\Omega^T_{*i}\{\eta_i^{-1} - 1 + i2\pi^{-1/2}\Omega^{1/2}(2\eta_i^{-1} - 3) \times [1 + (\omega_{ti}/\tilde{\omega}_{di})^2(1/4\Omega)]\}.$$

The imaginary part of $D(\Omega)$ is given by

$$\mathrm{Im}\, D(\Omega) \simeq \mathrm{Im}\, D_0(\Omega) \simeq -2\pi^{1/2}\Omega^{1/2}\exp(-\Omega) \times (\Omega^T_{*i} + \{1 - \Omega^T_{*i}[(\eta_i^{-1} - 1)/\Omega + 2]\} Y_r),$$

where $Y_r = \Omega^{1/2}\exp(-\Omega)\int_0^\Omega dz\, z^{-1/2}\exp z$. The corresponding Nyquist diagram for the unstable case is sketched in Fig. 1. Two requirements must be met in order for instability to take place: (i) $2\eta_i^{-1} - 3 < 0$, and (ii) $\mathrm{Re}\, D(\Omega_E) > 0$, where Ω_E is defined by the condition $\mathrm{Im}\, D(\Omega_E) = 0$ (cf. Fig. 1). The first of these imposes a criterion on η_i (i.e., $\eta_i > \frac{2}{3}$ or $\eta_i < 0$), while the second imposes a condition on Ω^T_{*i}, or equivalently, L_{Ti}/R. In general, the latter can only be determined numerically. Before discussing numerical results, we may gain further insight into the nature of the mode by looking at the nonresonant limit of the dispersion relation.

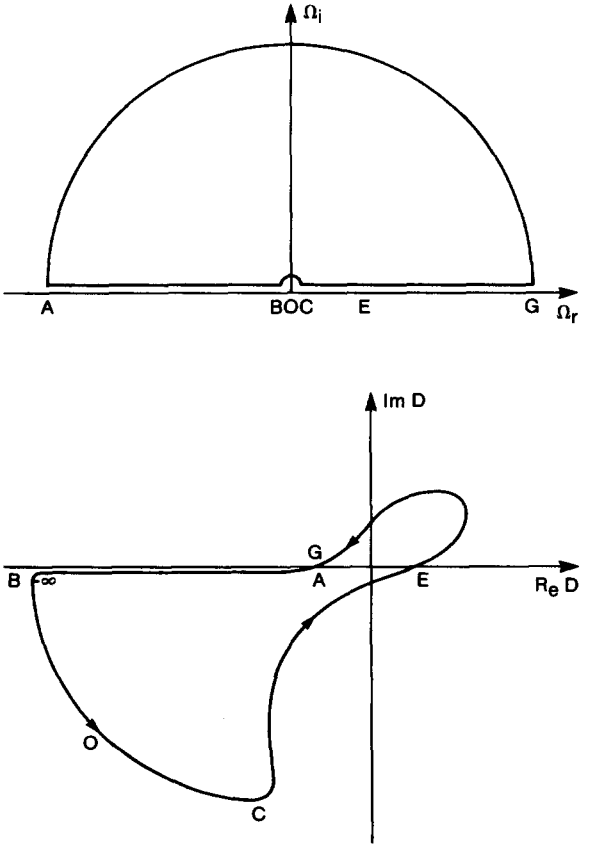

FIG. 1. Nyquist diagrams, featuring the unstable upper half frequency plane, and the image path in the D plane for instability.

A. Local nonresonant analysis

Expanding Eq. (3) in the limit of $\Omega > 1$, the leading-order radially local dispersion relation reduces to

$$1 + \frac{\tilde{\omega}_{de} - \omega_{*e}}{\omega} - \frac{[7\tilde{\omega}_{de}/4 - \omega_{*e}(1+\eta_i)]\tilde{\omega}_{de}}{\tau\omega^2} + \left(b_\perp - \frac{k_\parallel^2 v_{ti}^2}{2\omega^2}\right)\frac{\omega_{*e}(1+\eta_i)}{\omega} = 0. \tag{4}$$

It may be verified *a posteriori* that the validity condition for Eq. (4) is $1 > \epsilon^{1/2}$, and $1 > b_\perp > \epsilon/q^2$, where $\epsilon = r/R$ is the inverse aspect ratio. The first term in Eq. (4) is the adiabatic electron response. The second set of terms represents magnetic rotation; unlike MHD, these terms survive because the electrons respond differently than the ions, resulting in incomplete charge cancellation, and hence magnetic drift rotation. The third set of terms contains the stabilizing (since $\tilde{\omega}_{de} > 0$) contribution due to perpendicular compression, and the potentially destabilizing (i.e., $\omega_{*e}\tilde{\omega}_{de} > 0$) contribution due to adverse magnetic curvature. Finally, the last set of terms contain contributions resulting from finite ion Larmor radius and the uncompensated drift of compressed ions. The slablike branch can be recovered in the limit of $R \to \infty$ (i.e., $\tilde{\omega}_{de} \to 0$): $\omega_{sl}^2 \simeq -k_\parallel^2 v_{ti}^2(1+\eta_i)/2$. In this limit, the mode is driven unstable by parallel sound waves. This limit has been examined in detail elsewhere[14,15] and will not be pursued further in this work. The toroidal branch can be obtained by looking at the limit $k_\perp \rho_i > k_\parallel v_{ti}/(\omega_{*e}\tilde{\omega}_{de})^{1/2}$. Then, parallel compression can be treated perturbatively (i.e., $\omega = \omega_{tor} + \delta\omega_{tor}$) and to leading order,

$$2\omega_{tor} = [1 - b_\perp(1+\eta_i)]\omega_{*e} - \tilde{\omega}_{de} \pm \{[1 - b_\perp(1+\eta_i)]^2\omega_{*e}^2 + (1 + 7\tau^{-1})\tilde{\omega}_{de}^2 - 2[1 + 2\tau^{-1}(1+\eta_i)]\omega_{*e}\tilde{\omega}_{de}\}^{1/2}. \tag{5}$$

The stability of these modes is determined by the interplay of several dimensionless parameters: $b_\perp$, L_n/R, and L_{Ti}/R (also $\hat{s}/q$, as will be seen in the nonlocal analysis). It is misleading, therefore, to think of their stability simply in terms of the parameter η_i. Some general observations may nonetheless be made. First is the fact that depending on the wavelength and equilibrium gradients, the mode can reverse its sense of propagation from the electron to the ion direction. For instability—and hence transport—to occur without the inclusion of electron dissipation, these modes rotate in the ion direction. Second, it can be readily verified upon inspecting the radicand that for sufficiently steep density gradients, the mode is quenched, a feature that dovetails with the experimental observation of improved confinement with pellet injection. Rigorously, the Nyquist analysis of the full dispersion relation shows this critical value of η_i to be $\frac{2}{3}$. Third, we note that perpendicular compression exerts a stabilizing influence on the instability. The precise stability threshold will be taken up in Sec. IV. Finally, of potential relevance to the improved bulk confinement of H-mode discharges is the fact that for inverted density gradients, the threshold in η_i for instability to set in is enhanced. This can be seen upon noting that for inverted density gradients, both ω_{*e} and η_i change sign, so that the only source of destabilization now comes from the temperature gradient term, i.e., the last term in the radicand. The fastest growing mode is that associated with moderate wavelengths [i.e., $\epsilon^{1/2}/q < k_\perp \rho_i \sim (1+\eta_i)^{-1/2}$] and is given by

$$\gamma_{tor} \simeq \{[\tfrac{1}{2} + \tau^{-1}(1+\eta_i)]\omega_{*e}\tilde{\omega}_{de}\}^{1/2}. \tag{6}$$

Perturbatively, parallel compression results in a real frequency shift of magnitude $\delta\omega_{tor}/\omega_{tor} \simeq k_\parallel^2 v_{ti}^2 \omega_{*e}(1+\eta_i)/\omega_{tor}^2\Delta$, where Δ is the radical in Eq. (5). At marginality (i.e., $\Delta = 0$), parallel compression yields a stabilizing contribution given by $(\delta\omega_{tor}/\omega_{tor})^2 \simeq k_\parallel^2 v_{ti}^2 \omega_{*e}(1+\eta_i)/\omega_{tor}^3$, since then the mode is propagating in the electron direction.

B. Nonlocal analysis

The radially nonlocal theory is best implemented by exploiting the ballooning representation.[31] That is, we take note of the fact that in order to utilize their free energy source—unfavorable curvature—in the most efficient manner, these modes tend to localize about the magnetic field minimum and "balloon" outward. Expanding the nonresonant dispersion relation about this point, the eigenmode equation becomes

$$\left(A\frac{\partial^2}{\partial\vartheta^2} + B + C\vartheta^2\right)\hat{\phi} = 0, \tag{7}$$

where $-\infty < \vartheta < +\infty$ is a variable Fourier conjugate to the distance away from the mode rational surface in real space, and the true potential $\delta\phi$ is to be reconstructed in terms of an infinite sum of aperiodic quasimodes $\hat{\phi}(\vartheta)$. In the above,

$$A = (\omega_s^2\omega_{*e}/2\omega^3)(1+\eta_i),$$

$$B = \tau + \frac{\omega_{*e}}{\omega}\left[\tau\left(\frac{\tilde{\omega}_{de}}{\omega_{*e}} - 1\right) + b_\theta(1+\eta_i)\right] + \frac{\omega_{*e}\tilde{\omega}_{de}}{\omega^2}\left(1 + \eta_i - \frac{7\tilde{\omega}_{de}}{4\omega_{*e}}\right),$$

$$C = \frac{\omega_{*e}\, b_\theta \hat{s}^2}{\omega}\left\{1 + \eta_i + \frac{\tilde{\omega}_{de}}{\omega_{*e}}\frac{\hat{s} - \frac{1}{2}}{b_\theta\hat{s}^2} \times\left[\tau + \frac{\omega_{*e}}{\omega}\left(1 + \eta_i - \frac{7\tilde{\omega}_{de}}{2\omega_{*e}}\right)\right]\right\},$$

$\omega_s = c_s/qR$, $c_s^2 = 2T_e/m_i$ is the sound speed, and $b_\theta = (k_\theta \rho_i)^2/2$. In writing down Eq. (7), we have expanded the FLR term as $b_\perp = b_\theta(1 + \hat{s}^2\vartheta^2)$, and the nonlocal variation of the magnetic drift frequency as

$$G(\hat{s},\vartheta) = \cos\vartheta + \hat{s}\vartheta\sin\vartheta \simeq 1 + (\hat{s} - \tfrac{1}{2})\vartheta^2.$$

Equation (7) is the well-known Weber equation. The validity condition for this latter expansion is that the eigenmode decay within one oscillation of the potential well, i.e., $\epsilon^{1/2}/qb_\theta\hat{s} \lesssim \pi^2/4$. The eigenvalue condition is just $B = \pm i(2n+1)(AC)^{1/2}$, with n a non-negative integer, and where the lower sign must be chosen to satisfy causality. Assuming $(\hat{s} - \frac{1}{2})/\hat{s}^2 \ll b_\theta/\epsilon^{1/2}$, the lowest eigenvalue becomes

$$2\omega_{\rm tor} = [1 - b_\theta(1+\eta_i)]\omega_{*e} - \tilde{\omega}_{de} \pm \{[1 - b_\theta(1+\eta_i)]^2\omega_{*e}^2 + (1+7\tau^{-1})\tilde{\omega}_{de}^2 - 2[1+2\tau^{-1}(1+\eta_i) \times (1+i\hat{s}/\sqrt{2}q)]\omega_{*e}\tilde{\omega}_{de}\}^{1/2}. \quad (8)$$

The lowest eigenmode now has a growth rate

$$\omega_{\rm tor} \simeq i\{[\tfrac{1}{2} + \tau^{-1}(1+\eta_i)(1+i\hat{s}/\sqrt{2}q)]\omega_{*e}\tilde{\omega}_{de}\}^{1/2}. \quad (9)$$

The limit of $\hat{s}/q < 1$ recovers the result obtained from the local analysis. The corresponding radial mode width is given by

$$(k_r\rho_i)^2 = \sqrt{2}(\hat{s}/q)(\tilde{\omega}_{de}/|\omega_{\rm tor}|). \quad (10)$$

C. Transport

We finally turn our attention to estimating the level of heat and particle transport expected to evolve from these modes. A proper evaluation of the transport coefficients requires a steady-state solution of the field evolution equations while fully taking account of the destabilizing source ("stirring"), dissipation, and transfer between these two ranges (regulated by turbulent $\mathbf{E}\times\mathbf{B}$ advection). The result of such analyses in the past has been to recover the scaling predictions of a *proper* mixing-length theory (we shall discuss shortly what we mean by "proper"), but with a slowly varying multiplier. The latter physically takes account of the sum over all scales over which the local mixing-length theory holds, weighted by how strongly each scale is excited. The analysis required to recover this multiplier is often involved and lengthy. Short of such a detailed nonlinear analysis, we may turn profitably to mixing-length theory if we are prepared to content ourselves with the more modest goal of uncovering the local parameter scalings. In this endeavor, it is more illuminating to work within the context of fluid equations.

We write down the dominant balances at steady state (i.e., $\partial/\partial t = 0$) in the vorticity, parallel momentum, and pressure equations:

$$\nabla\cdot\mathscr{D}_k\nabla\nabla^2\Phi \sim i\hat{\mathbf{e}}_\parallel\cdot\nabla V_\parallel + i\omega_{de}(\rho_s/c_s)\Pi, \quad (11)$$

$$\nabla\cdot\mathscr{D}_k\nabla V_\parallel \sim i\hat{\mathbf{e}}_\parallel\cdot\nabla(\Phi+\Pi), \quad (12)$$

$$\nabla\cdot\mathscr{D}_k\nabla\Pi \sim i\omega_{*e}(\rho_s/c_s)[(1+\eta_i)/\tau]\Phi, \quad (13)$$

where $\Phi = e\delta\phi/T_e$ is the normalized fluctuations, $V_\parallel = \delta v_\parallel/c_s$ is the normalized parallel velocity fluctuations, $\Pi = \delta p_i/P_i$ is the normalized pressure fluctuations, $P_i = n_iT_i$ is the equilibrium pressure, and all length scales have been normalized to $\rho_s = c_s/\Omega_{ci}$. In writing down Eqs. (11)–(13), we have employed experience gleaned from renormalized perturbation theory to write the transfer terms ($\mathbf{E}\times\mathbf{B}$ advective nonlinearities) as turbulent diffusion operators,

$$\mathscr{D}_k = \sum_{k',\omega'} g_{k',\omega'}(k'\rho_s)^2\langle\Phi\rangle_{k'}^2, \quad (14)$$

where $g_{k',\omega'}$ is the appropriate renormalized propagator, and where $\langle\cdots\rangle$ represents a spectral average. Here, $\mathscr{D}_k$ is normalized to the Bohm diffusivity $D_B = \rho_sc_s$. The left-hand side of Eqs. (11)–(13) represents the turbulent mixing of vorticity, parallel momentum, and pressure, respectively. The terms on the right-hand side of Eq. (11) represent parallel compression and curvature drive, respectively. The right-hand of Eq. (12) represents the acceleration resulting from the parallel electric field and the parallel pressure gradient. Finally, the right-hand side of Eq. (13) represents the advection of equilibrium pressure by the fluctuating $\mathbf{E}\times\mathbf{B}$ drift. Writing the radial correlation length as Δ_k, we invoke two asymptotic balances in order to determine the transport scalings. The first is a balance between the turbulent mixing of pressure over a nonlinear mode width with the curvature drive. This gives

$$\mathscr{D}_k \sim (\rho_s/c_s)[\tilde{\omega}_{de}\omega_{*e}(1+\eta_i)]^{1/2}\Delta_k^2. \quad (15)$$

In writing down Eq. (15), we have taken account of the spatial variation of the magnetic drift frequency [i.e., $G(\hat{s},\vartheta)$]. The second asymptotic balance, which determines the radial correlation (or mixing) length, is between vorticity diffusion and parallel compression:

$$\Delta_k \sim [(q/\hat{s})(R/k\rho_s^2)\mathscr{D}_k]^{1/4}. \quad (16)$$

Substituting for $\mathscr{D}_k$ from Eq. (15) into Eq. (16), we obtain an expression for the mixing length at which saturation occurs:

$$\Delta_k \sim \left(\frac{q^2}{\hat{s}^2}\frac{\omega_{*e}}{\tilde{\omega}_{de}}\frac{1+\eta_i}{\tau}\right)^{1/4}. \quad (17)$$

Note that this is at odds with the oft-invoked assumption[30] of spatial isotropy ($k_r = k_\theta$), which fails to take account of the ballooning structure of the toroidal ion-pressure-gradient-driven drift waves ($k_r > k_\theta$), and consequently yields erroneous expressions for the transport coefficients. The level of diffusion necessary to maintain a dynamical balance between turbulent transfer of energy and curvature drive is then

$$\mathscr{D}_k \sim \frac{q}{\hat{s}}\frac{k\rho_s^2}{L_n}\frac{1+\eta_i}{\tau}. \quad (18)$$

The level of potential fluctuations (and hence through quasi-neutrality, density fluctuations) can be obtained upon substituting the expression for $\mathscr{D}_k$ into Eq. (14), yielding

$$\frac{\delta n}{n_0} = \frac{e\delta\phi}{T_e} \sim \left(\frac{q}{\hat{s}}\right)^{1/2}\frac{\rho_s}{L_n}\left(\frac{\tilde{\omega}_{de}}{\omega_{*e}}\right)^{1/4}\left(\frac{1+\eta_i}{\tau}\right)^{3/4}. \quad (19)$$

The pressure fluctuations are related to the potential fluctuations through

$$\frac{\delta p}{P_i} \sim \left(\frac{\omega_{*e}}{\tilde{\omega}_{de}}\frac{1+\eta_i}{\tau}\right)^{1/2}\frac{e\delta\phi}{T_e}.$$

It is important to note that the level of pressure fluctuations can be substantially higher than that of potential fluctuations. The physical reason for this is that since the instability under consideration is essentially driven by the temperature gradient, the level of temperature fluctuations significantly exceeds that of density fluctuations, i.e., $\delta p_i/P = \delta n_i/n_0 + \delta T_i/T_i \gg \delta n_i/n_0 = e\delta\phi/T_e$. Thus the choice of potential fluctuations as the mixing field within the context of the present problem, as sometimes done in the past,[28] is incorrect and leads to erroneous results. Using Eq. (19), we may now obtain an expression for the rms pressure fluctuations:

$$\frac{\delta p}{P_i} \sim \left(\frac{q}{\hat{s}}\right)^{1/2} \frac{\rho_s}{L_n} \left(\frac{\omega_{*e}}{\tilde{\omega}_{de}}\right)^{1/4} \left(\frac{1+\eta_i}{\tau}\right)^{5/4}. \tag{20}$$

The radial heat flux is given by $Q_i = \langle \delta v_r \, dp \rangle$, where δv_r is the turbulent radial velocity. Substituting from Eqs. (19) and (20), we have

$$Q_i \sim \frac{q}{\hat{s}} \frac{k \rho_s^3 c_s}{L_n^2} \left(\frac{1+\eta_i}{\tau}\right)^2 P_i. \tag{21}$$

The ion thermal diffusivity is then given by

$$\chi_i = \frac{Q_i}{dP_i/dr} \sim \frac{q}{\hat{s}} \omega_{*e} \rho_s^2 \frac{1+\eta_i}{\tau}. \tag{22}$$

These expressions are, of course, only valid for $\eta_i > \eta_{i,\mathrm{cr}}$. Three features of Eq. (22) are noteworthy. First is the proportionality of χ_i with k_θ. That thermal transport is more severe at shorter wavelengths than at long is a direct consequence of the more rapid rate of decorrelation between waves and particles as one progresses to smaller scales. Already from the result of the linear analysis, we can impose an upper bound on $k_\theta \rho_i$ of $(1+\eta_i)^{-1/2}$. A more confident upper bound awaits a fully nonlinear theory. Second is the fact that the expression for the thermal diffusivity evinces an intrinsically local inverse linear scaling with current (through the q dependence). This feature may be of relevance to experimental inferences of such scaling if, as discussed in the Introduction, they were to be borne out for the ion channel alone. There are caveats to this statement, a discussion of which we will postpone to the Conclusion. Finally, as is already apparent from the dependence of the heat diffusivity on bulk gradients, it should be noted that the level of transport is quite severe for $\eta_i > \eta_{i,\mathrm{cr}}$. The implication is that equilibrium profiles will have a strong tendency to remain close to marginality with respect to ion-pressure-gradient-driven modes. We will return to this point in the Conclusion.

While directly responsible for the degradation of the ion channel, ion-pressure-gradient-driven turbulence can also induce enhanced particle and heat loss through the electron channel. In the bulk region of the plasma, dissipative trapped electron modes are expected to be the dominant loss mechanism for the electrons. The nonadiabatic piece of the trapped electron distribution function is given by

$$\delta h_{te} \simeq i \frac{e\delta\phi}{T_e} \frac{\omega - \omega_{*e}\left[1+\eta_e(v^2/v_{te}^2 - \frac{3}{2})\right]}{\nu_e/\epsilon} F_{\mathrm{Me}},$$

where ν_e is the electron collision frequency. An estimate of the radial particle and electron heat flux can then be obtained as

$$\begin{pmatrix} \Gamma_e \\ Q_e \end{pmatrix} = \int_{\mathrm{tr}} d^3v \begin{pmatrix} 1 \\ m_e v^2/2 \end{pmatrix} \langle \delta v_r \, \delta f_e \rangle$$
$$\sim \begin{pmatrix} 1 \\ 3T_e(1+\eta_e)/2 \end{pmatrix} \epsilon^{3/2} n_0 \rho_s \times \frac{(\omega_{*e}^3 \omega_{de})^{1/2}}{\nu_e} \frac{q}{\hat{s}} \frac{\rho_s}{L_n} \left(\frac{1+\eta_i}{\tau}\right)^{3/2}, \tag{23}$$

from which follows

$$\mathscr{D}_e \sim \chi_e \sim \left[(\omega_{*e}\omega_{de})^{1/2}/\nu_e\right] \left[(1+\eta_i/\tau)\right]^{1/2} \chi_i, \tag{24}$$

where $\mathscr{D}_e$ is the particle diffusion coefficient. As pointed out in Ref. 14, χ_e and χ_i have quite different scalings, and, although they may be of comparable magnitude in specific instances, it is, in general, quite misleading to arbitrarily assume them to be equal.

It is of interest to compare the expressions for the fluctuations and transport coefficients obtained here to corresponding ones for the slab branch.[14,15] Insofar as the density fluctuations are concerned, the slab branch exhibits a stronger dependence on η_i than the toroidal branch. Insofar as the thermal diffusivities are concerned, both branches exhibit identical scalings with the safety factor and shear. In order of magnitude,

$$\frac{\chi_i^{\mathrm{sl}}}{\chi_i^{\mathrm{tor}}} \sim \frac{R}{L_n} \frac{1+\eta_i}{\tau}. \tag{25}$$

For moderate aspect ratios, *there is no sound basis for distinguishing between the two experimentally*, especially since equilibrium profiles can be expected to be pinned near their marginal values. Indeed, regardless of the aspect ratio, one branch or the other of the ion-pressure-gradient-driven mode will survive.

Finally, we may proceed to look at the scaling of the energy confinement time with parameters of interest. However, the very notion of using a *local* expression for the heat diffusivity in deriving the energy confinement time, and then comparing the result with experimentally inferred scalings which in turn depend on *global* parameters, is not only untrustworthy, but can also be very misleading. For this reason, *we deliberately eschew such an analysis.*

III. TRAPPED-ION ∇p_i-DRIVEN MODE

As plasma parameters push into the low collisionality regime, ion trapping can no longer be ignored and needs to be accounted for in the stability and transport analysis. The relevant frequency ordering is now given by

$$\omega_{bi}, \omega_{ti} \gg \omega_{*i} > |\omega| \gtrsim \tilde{\omega}_{di}, \nu_{\mathrm{eff},i},$$

where $\nu_{\mathrm{eff},i} \sim \nu_i/\epsilon$ is the effective ion collision frequency. Consider first the "collisionless" trapped-ion branch. The toroidal ion-pressure-gradient-driven branch of Sec. II C smoothly connects onto this branch as we go to longer wavelengths (i.e., $k_\theta \rho_i < \epsilon^{3/4}/q$). The essential difference between the two modes is that parallel compression (and hence, shear damping) and the spatial variation of the magnetic drift frequency are removed from the analysis upon bounce averaging of the drift kinetic equation. The dispersion relation is then given by

$$\frac{1+\tau^{-1}}{2\sqrt{2\epsilon}} + \frac{\overline{\omega}_{de} - \omega_{*e}}{\omega} \frac{[7\overline{\tilde{\omega}}_{de}/4 - \omega_{*e}(1+\eta_i)]\overline{\omega}_{de}}{\tau\omega^2} + b_\perp \frac{\omega_{*e}(1+\eta_i)}{\omega} = 0, \tag{26}$$

where $\overline{(\cdots)} = \oint dl(\cdots)/v_\parallel$ denotes a bounce average, and $2\sqrt{2\epsilon}$ is the fraction of trapped particles. In writing down Eq. (26), we have ignored the circulating-ion response, as well as the distinction between $\delta\phi$ and $\overline{\delta\phi}$. The fastest growing mode now becomes

$$\gamma_{\rm tr} \simeq (\sqrt{2\epsilon}\{[1+2(1+\eta_i)/\tau]/(1+\tau^{-1})\}\omega_{*e}\bar{\omega}_{de})^{1/2}. \tag{27}$$

Because of the fact that parallel compression is removed by bounce averaging, the radial mode width is given by $(k_\theta \hat{s})^{-1}$, so that the simple mixing-length expression for the thermal diffusivity is

$$\chi_i \sim (k_\theta \hat{s})^{-2}\left[\sqrt{2\epsilon}\,\omega_{*e}\bar{\omega}_{de}(1+\eta_i/\tau)\right]^{1/2}. \tag{28}$$

Comparing this expression with the corresponding one for the toroidal η_i mode, we have

$$\chi_i^{\rm tr}/\chi^{\rm tor} \sim \epsilon^{3/4}/q\hat{s}(k_\theta \rho_i)^2,$$

which can significantly exceed unity at long wavelengths. A natural upper bound on the wavelength is imposed by the requirement that $\nu_{{\rm eff},i}$ not be greater than $\gamma_{\rm tr}$.

From Eq. (26), it is clear that to have instability, one must satisfy the condition

$$\frac{2(1+\tau^{-1})}{\sqrt{2\epsilon}}\,\frac{1+\eta_i}{\tau} > \frac{\omega_{*e}}{\bar{\omega}_{de}}, \tag{29}$$

yielding a critical η_i on the order of $\epsilon^{-1/2}$. If Eq. (29) is violated, then the trapped-ion mode becomes purely oscillatory. In previous work[18] with the influence of temperature gradients ignored (i.e., $\eta_i = 0$), it was noted that this so-called dissipative trapped-ion mode, which now propagates in the electron direction, is destabilized by electron collisions, while ion collisions have a stabilizing influence. We note here that for η_i above a certain threshold, ion collisions can also have a *destabilizing* influence.

In the banana regime of interest here, pitch angle scattering dominates over scattering in energy. If we were to add to the drift kinetic equation a linearized pitch angle scattering collision operator of the form

$$C(\delta h_i) = 2\nu_i\left(\frac{E}{T_i}\right)^{-3/2}\frac{(1-\lambda B)^{1/2}}{B}\frac{\partial}{\partial\lambda} \times\left(\lambda(1-\lambda B)^{1/2}\frac{\partial \delta h_i}{\partial\lambda}\right),$$

where $\lambda = \mu/E$ is the pitch angle variable, it is easy to see by balancing terms that a boundary layer in pitch angle is formed between trapped and circulating ions of width

$$\Delta\lambda \sim \left(\frac{1}{B_{\rm min}} - \frac{1}{B_{\rm max}}\right)\left(\frac{\nu_{{\rm eff},i}(E)}{\omega}\right)^{1/2},$$

with $\nu_{{\rm eff},i} \sim \nu_i E^{-3/2}/\epsilon$. The collisional contribution to the dispersion relation can be estimated using variational techniques.[32] The result is

$$\delta\omega \simeq -i\int dE\, E^{1/2}\left(\frac{\nu_{{\rm eff},i}(E)}{\omega}\right)^{1/2}\omega_{*e}^{t}(E)F_{{\rm M}i}. \tag{30}$$

Noting that $\nu_{{\rm eff},i} \propto E^{-3/2}$, the energy integrals may be straightforwardly evaluated to find that the dissipative contribution is proportional to $(1-3\eta_i/4)$. We conclude therefore that the trapped-ion branch remains unstable for $\eta_i > \frac{4}{3}$ and $\nu_i < \epsilon^{5/4}\omega_{*e}\bar{\omega}_{de}$.

Assuming these limits, we may provide an estimate of the ion thermal diffusivity:

$$\chi_i \sim \frac{\epsilon^{5/4}}{\hat{s}^2\nu_i}\frac{\rho_s^2 c_s^2}{L_{Ti}R}. \tag{31}$$

As is characteristic of trapped-ion modes, the predicted level of thermal diffusion is both very large in magnitude and very unfavorable in temperature scaling ($\chi_i \propto T^{7/2}$), thus indicating a probable strong tendency for η_i to be forced below $\frac{4}{3}$ in the collisionless regime.[21] An important point to notice from both Eqs. (28) and (31) is that since $\chi_i^{\rm tr} \propto \hat{s}^{-2}$, a saturation of the heretofore experimentally observed favorable current scaling of τ_E may be anticipated for low ion-collisionality discharges.

IV. FLAT-DENSITY LIMIT

One of the most conspicuous features of H-mode plasmas is the very flat electron density profile over the bulk of the discharge. Assuming the ion density profile is about as flat as the electron density profile (this depends on the impurity and energetic-species profile), η_i goes to infinity, and one might naively predict that thermal transport processes intensify, a conclusion incompatible with experimental observations. A more careful analysis, however, shows that the relevant stability parameter in this flat-density limit is L_{Ti}/R, i.e., the ratio of the ion temperature gradient length scale to the toroidal curvature radius, rather than $\eta_i = L_n/L_{Ti}$.[28] More recently, Dominguez and Waltz have made the suggestion, based on a fluid analysis, that perpendicular compression can completely stabilize the ion-temperature-gradient-driven mode.[29] The stabilizing influence identified as resulting from perpendicular compressibility by these authors, however, is in fact a result of the leftover piece of the magnetic drift frequency caused by incomplete charge cancellation between electrons and ions. Perpendicular compression does indeed have a stabilizing influence, but as we shall show here, is unlikely to provide complete stabilization, at least within the validity limitations of ignoring finite sound effects.

To see why there can be little confidence in the predictions of the nonresonant (or fluid) theory, it suffices to take the $\eta_i \to \infty$ limit of the nonresonant dispersion relation derived in Sec. II A:

$$2\omega/\tau\omega_{*i}^{T} \simeq b_\perp + \epsilon_{Ti} \pm [(1+7\tau^{-1})\epsilon_{Ti}^2 - 4\tau^{-1}\epsilon_{Ti}]^{1/2}, \tag{32}$$

where $\omega_{*i}^{T} = -k\rho_i v_{ti}/L_{Ti}$, and $\epsilon_{Ti} = L_{Ti}/R$. Although for $\epsilon_{Ti} > 4/(7+\tau)$ the mode is stabilized, the expansion in ω_{di}/ω which was used to obtain Eq. (2) breaks down, since then $\omega \sim \epsilon_{Ti}\,\omega_{*i}^{T} \sim \omega_{di}$.

It is therefore necessary to go back to the resonant dispersion relation, Eq. (3), and look for marginal stability [corresponding to Re $D(\Omega_E) = 0$ in the Nyquist analysis]. As mentioned in Sec. II, this is possible only numerically. Such a numerical analysis has been carried out, and the result plotted in Fig. 2. The threshold value obtained for $b_\perp = k_\parallel = 0$ is $L_{Ti}/R \simeq 0.35$. Thus for a typical aspect ratio of 3, the stability condition becomes $L_{Ti}/a \geqslant 1.05$, which is obviously never satisfied over the entire discharge. In contrast to Dominguez and Waltz,[29] therefore, we conclude that barring the possibility that finite Larmor radius and sound corrections would significantly reduce the threshold, the flat-density theory of ion-temperature-gradient-driven modes does not predict a dramatic improvement in the ion

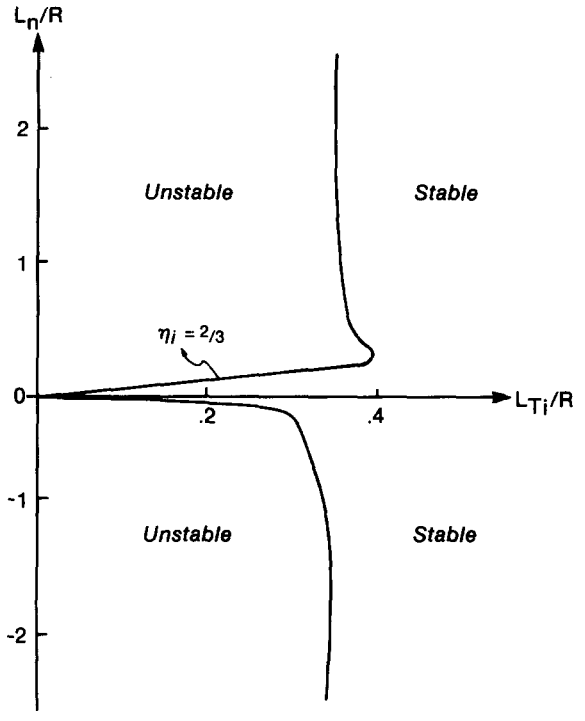

FIG. 2. Stability diagram in L_n vs L_{Ti} space.

channel in the good confinement zone of H-mode discharges where it is applicable. The electron channel, on the other hand, can be dramatically improved by profile flattening in this zone.

V. ENERGETIC TRAPPED-PARTICLE EFFECTS

An undesirable consequence of auxiliary heating has been an almost universally observed degradation in confinement with increasing input power, at least in the L-mode regime of operation. Since many of the proposed heating schemes (e.g., ICRF, ECRH, perpendicular neutral beam injection) produce a profusion of energetic trapped particles, it becomes necessary to ask how these particles interact with the background species and affect plasma instabilities. The importance of trapped particles, insofar as stability analysis goes, lies in the fact that they predominantly undergo unfavorable drifts. This unfavorable drift can therefore be expected to provide an additional source of free energy for curvature-driven instabilities.[34–37] We are then led to ask what influence such a population of unfavorably drifting energetic species has on the stability of toroidal ion-pressure-gradient-driven drift modes.

Our frequency ordering is given by $\omega_{bh} \gg |\omega| \gg \omega_{bi}$. To get a qualitative feel for their influence, we model the energetic species as a Maxwellian distribution at high temperature (i.e., $T_h \gg T_i$, where the subscript "h" refers to the hot particles) and low density (i.e., $n_h \ll n_i, n_e$). This is a reasonable model for those energetic particles created during radio frequency heating, as these undergo something akin to a random walk, wherein they suffer a kick after every excursion close to the banana tip, and this kick may be in either direction. Further, we consider only the nonresonant limit (i.e., $|\omega| \gg \bar{\omega}_{dh}$) of these modes. This assumption is unlikely to be realized in practice; however, it suffices to bring out the qualitative features of the instability. The resonant limit will be explored in a future publication. The resulting dispersion relation is

$$\frac{n_{0e}}{T_e} = \frac{n_{0i}}{T_i}\left[\frac{\bar{\omega}_{di}-\omega_{*i}}{\omega} + \frac{[7\bar{\omega}_{di}/4 - \omega_{*i}(1+\eta_i)]\bar{\omega}_{di}}{\omega^2} + \left(b_{\perp i} - \frac{k_\parallel^2 c_s^2}{2\omega^2}\right)\frac{\omega_{*i}(1+\eta_i)}{\omega}\right] + \frac{n_{0h}}{T_h}\left[-1 + 2\sqrt{2\epsilon}\left(1 + \frac{\bar{\omega}_{dh}-\omega_{*h}}{\omega} + \frac{[7\bar{\omega}_{dh}/4 - \omega_{*h}(1+\eta_h)]}{\omega^2} + b_{\perp h}\frac{\omega_{*h}(1+\eta_h)}{\omega}\right)\right], \quad (33)$$

where the notation is a standard generalization of preceding sections. Note that from quasineutrality

$$n_e = n_i + n_h,$$

$$\frac{dn_{0e}}{dr} = \frac{dn_{0i}}{dr} + \frac{dn_{0h}}{dr}.$$

Thus the dispersion relation is the solution to the quadratic algebraic equation

$$\frac{n_{0e}}{n_{0i}\tau_e}\Omega^2 - \left(1 - b_{\perp i}(1+\eta_i) - \epsilon_i + 2\sqrt{2\epsilon}\frac{L_{ni}n_{0h}}{L_{nh}n_{0i}} \times [1 - b_{\perp h}(1+\eta_h) - \epsilon_h]\right)\Omega + \epsilon_i\left(1 + \eta_i - \frac{7}{4}\epsilon_i\right) + 2\sqrt{2\epsilon}\left(\frac{L_{ni}}{L_{nh}}\right)^2\frac{\beta_h}{\beta_i}\epsilon_h\left(1 + \eta_h - \frac{7}{4}\epsilon_h\right) = 0, \quad (34)$$

where $\Omega = -\omega/\omega_{*i}$, $\epsilon_j = L_{nj}/R$, and $\beta = p/B^2$ is the species beta content. We note that for strongly localized heat deposition profiles, $L_{nh} \ll L_{ni}$, energetic particles can substantially exacerbate the instability.

VI. DISCUSSION AND SUMMARY

In a recent work,[21,22] we explored the nonlinear evolution of the resonantly destabilized ($\bar{\omega}_{di} \gg |\omega| \simeq \bar{\omega}_{di}$) trapped-ion-temperature-gradient-driven instability. The present investigation complements that work by investigating the nonresonant limit ($\omega \gg \bar{\omega}_{di}$) of the same instability, as well as the moderate-wavelength ($|\omega| \sim \omega_{di} \gg \omega_{ti}$) branch of the same family of instabilities. The so-called "ubiquitous mode" of Coppi[28] is the short-wavelength branch ($b_\perp \gg 1$) of these instabilities. When juxtaposed with the slablike branch,[14,15] we have thus provided a unified account of electrostatic ion-pressure-gradient-driven drift wave instabilities and transport over all parameter regimes. It is important to note that this family of instabilities is quite robust, in the sense that at least one branch or another is likely to persist upon changing bulk parameters. In particular, as is indicated by Eq. (25), while increasing the aspect ratio can have a favorable influence in reducing the population of trapped particles, this benefit comes only at the expense of aggravat-

TABLE I. Compendium of relevant scalings for ion-pressure-gradient-driven modes.

	Slab[12,13]	Toroidal	Trapped Ion
$k_\theta \rho_i$	$(1+\eta_i)^{-1/2} > k_\theta \rho_i > \epsilon^{1/2}/q$	$(1+\eta_i)^{-1/2} > k_\theta \rho_i > \epsilon^{1/2}/q$	$k_\theta \rho_i < \epsilon^{3/4}/q$
γ/ω_{*e}	$\dfrac{1+\eta_i}{\tau}$	$\left(\dfrac{\tilde{\omega}_{de}}{\omega_{*e}}\dfrac{1+\eta_i}{\tau}\right)^{1/2}$	$\left(\sqrt{2\epsilon}\dfrac{\bar{\omega}_{de}}{\omega_{*e}}\dfrac{1+\eta_i}{\tau}\right)^{1/2}$
$\Delta x/\rho_s$	$\left(\dfrac{qR}{\hat{s}L_n}\dfrac{1+\eta_i}{\tau}\right)^{1/2}$	$\left[\left(\dfrac{q}{\hat{s}}\right)^2\dfrac{\omega_{*e}}{\tilde{\omega}_{de}}\dfrac{1+\eta_i}{\tau}\right]^{1/4}$	$(k_\theta \rho_s \hat{s})^{-1}$
$\delta n/n$	$\left(\dfrac{qR}{\hat{s}L_n}\right)^{1/2}\left(\dfrac{1+\eta_i}{\tau}\right)^{3/2}\dfrac{\rho_s}{L_n}$	$\left(\dfrac{q}{\hat{s}}\right)^{1/2}\left(\dfrac{1+\eta_i}{\tau}\right)^{3/4}\left(\dfrac{\tilde{\omega}_{de}}{\omega_{*e}}\right)^{1/4}\dfrac{\rho_s}{L_n}$	$\dfrac{(2\epsilon)^{1/4}}{k_\theta \hat{s} L_n}\left(\dfrac{\bar{\omega}_{de}}{\omega_{*e}}\dfrac{1+\eta_i}{\tau}\right)^{1/2}$
$\dfrac{\chi_i}{\omega_{*e}\rho_s^2}$	$\dfrac{qR}{\hat{s}L_n}\left(\dfrac{1+\eta_i}{\tau}\right)^2$	$\dfrac{q}{\hat{s}}\dfrac{1+\eta_i}{\tau}$	$\dfrac{(2\epsilon)^{1/4}}{b_\theta \hat{s}^2}\left(\dfrac{\bar{\omega}_{de}}{\omega_{*e}}\dfrac{1+\eta_i}{\tau}\right)^{1/2}$
$\dfrac{\chi_e \sim \mathscr{D}_e}{\omega_{*e}\rho_s^2}$	$\epsilon^{3/2}\dfrac{qR}{\hat{s}L_n}\dfrac{\omega_{*e}}{\nu_e}\left(\dfrac{1+\eta_i}{\tau}\right)^3$	$\epsilon^{3/2}\dfrac{q}{\hat{s}}\dfrac{(\omega_{*e}\tilde{\omega}_{de})^{1/2}}{\nu_e}\left(\dfrac{1+\eta_i}{\tau}\right)^{3/2}$	$\epsilon^2\dfrac{\bar{\omega}_{de}}{b_\theta \hat{s}^2 \nu_e}\dfrac{1+\eta_i}{\tau}$

ing the slablike branch of these modes. Perhaps alarmingly, the theory suggests a possible saturation of the heretofore favorable scaling with current as plasma discharges approach very low collisionality regimes. A partial summary of our results is displayed in Table I. Note that all expressions are well behaved in the limit of $L_n \to \infty$.

In the process of this study, several of the experimental features discussed in the Introduction were addressed. Of potential significance is the issue of current scaling. The transport coefficients of Sec. II evince an intrinsically local inverse linear scaling with current. It has been suggested,[39] however, that the shear parameter scales as $q(a)$, so that the scaling with current may not be a strong one. A key clue to the source of the current scaling may be the experimental observation that profiles are found to hover about marginality. As was hinted in Refs. 22 and 33, there may in fact be no *intrinsically local* current scaling at all, but rather that profiles in the bulk of the discharge remain marginal with respect to ion-pressure-gradient-driven modes, and that transport processes in the edge, such as resistive fluid turbulence, dynamically couple in to the center of the discharge and thus determine the transport scalings. Such a scenario is both compatible with experimental observations and removes several of the shortcomings of drift wave scalings, such as unfavorable current and favorable temperature scaling. It also reproduces the experimentally observed unfavorable power scaling. Work on this front is in progress and will be reported in a forthcoming publication.

In the meantime, more experimental evidence would be welcome in helping to sort out among these various alternatives. A definitive experiment in favor of or against an *intrinsic* current scaling would be most valuable in this regard. Such an undertaking would require detailed ion temperature profile measurements, coupled with observations of heat pulse propagation, which could then be used in power balance calculations to determine the radially local parameter scalings of the ion heat flux. Scaling laws for the ion heat flux are generally much less unreliable and hence more useful theoretically than scalings for the thermal diffusivity and energy confinement time. This is because the asymmetric terms of the transport matrix are likely to contribute to the expression for the thermal flux, a feature often ignored in power balance calculations. That empirically fitted energy confinement time scaling laws are not useful from a theoretical point of view follows from the fact that such scalings depend on *global* parameters, whereas theory generally predicts *local* scalings of transport coefficients, so that a comparison between the two may be, at worst, superfluous, and at best, misleading.

More generally, the improvement in confinement with pellet injection resulting from profile steepening suggests the use of the latter as an active diagnostic tool. FIR scattering diagnostics afford one an invaluable aid in identifying the isotope and current scaling in the radial correlation length [cf. Eq. (17)]. With regard to the improved bulk confinement of H-mode discharges, two experimental results would significantly aid theoretical attempts at understanding the source of the improvement. First, it needs to be checked whether the improvement comes about in the electron channel or ion channel, or both. This should be possible with transport simulations, coupled with electron *and* ion temperature profile measurements. *Inferences drawn without the availability of ion profiles cannot be considered conclusive.* Second, a careful look at the *ion* density profiles would be most helpful.

ACKNOWLEDGMENTS

Useful discussions with Dr. R. Waltz and Dr. R. R. Dominguez are gratefully acknowledged.

This work was supported by the U.S. Department of Energy Contracts No. DEFG03-85ER53199, No. DE-FG03-88ER53275, No. DE-AC03-84ER53158, and No. DE-AT03-84ER53158.

APPENDIX: DERIVATION OF THE DISPERSION RELATION

In this appendix, we outline the derivation of Eq. (3). The dispersion relation is given by

$$D(\Omega) = -(1+\tau^{-1}) + \pi^{-1/2}\int d\bar{v}_\perp^2\, d\bar{v}_\parallel\, \delta h_{ic}.$$

Using Eq. (2), we may write this as

$$D(\Omega) = -(1+\tau^{-1}) + \{\Omega - \Omega^{T}_{*i}[(\eta_i^{-1} - \tfrac{3}{2}) - (\partial_\alpha + \partial_\beta)]\} \times [1 + b_\perp \partial_\beta - \tfrac{1}{2}(\omega_{ti}/\tilde{\omega}_{di})^2 \partial_\Omega^2 \partial_\alpha] F_{\alpha,\beta}|_{\alpha,\beta=1}, \quad \text{(A1)}$$

where

$$F_{\alpha,\beta} = -i\pi^{-1/2} \int_0^\infty d\lambda \int d\bar{v}_\perp^2 \, d\bar{v}_\parallel \times \exp\left[-\alpha v_\parallel^2 - \beta v_\perp^2 + i\lambda\left(\Omega - \bar{v}_\parallel^2 - \frac{v_\perp^2}{2}\right)\right] = -i\int_0^\infty d\lambda \frac{\exp(i\lambda\Omega)}{(\alpha + i\lambda)^{1/2}(\beta + i\lambda/2)}. \quad \text{(A2)}$$

By integrating the differential equation, $F_{\alpha,\beta}$ may be written in a more compact form,

$$\frac{\partial F_{\alpha,\beta}}{\partial \Omega} + 2\beta F_{\alpha,\beta} = 2\Omega^{-1/2}\exp(-\Omega)\int_{-\infty}^{\Omega} dz\, z^{-1/2}\exp z,$$

which it can easily be shown to satisfy. One obtains

$$F_{\alpha,\beta} = 2\exp(-2\beta\Omega)\int_{-\infty}^{\Omega} dy\, y^{-1/2} \times \exp[(2\beta-1)y]\int_{\infty}^{y} dz\, z^{-1/2}\exp z. \quad \text{(A3)}$$

Differentiating Eq. (A3) with respect to β and rearranging terms, an expression for $\partial_\beta F_{\alpha,\beta}$ can be derived:

$$\partial_\beta F_{\alpha,\beta} = -[2/(2\beta-1)]\{[\Omega(2\beta-1) + \tfrac{1}{2}] F_{\alpha,\beta} - 2Y + 1/\beta\}, \quad \text{(A4)}$$

where

$$Y = (\Omega F_{1,1})^{1/2} = \Omega^{1/2}\exp(-\Omega)\int_{-\infty}^{\Omega} dz\, z^{-1/2}\exp z.$$

Having obtained $\partial_\beta F_{\alpha,\beta}$, all other needed derivatives can be obtained:

$$\partial_\alpha F = 1 - \Omega F - \tfrac{1}{2}\partial_\beta F,$$
$$\partial_\beta^2 F = -2(\Omega + \tfrac{1}{2})\partial_\beta F + 2F - 8Y + 6,$$
$$\partial_{\alpha\beta} F = -1 - \Omega\partial_\beta F - \tfrac{1}{2}\partial_\beta^2 F,$$
$$\partial_\alpha^2 F = \Omega(Y^2 - 1 + \partial_\beta F) + \tfrac{1}{4}\partial_\beta^2 F,$$

where all expressions have been evaluated at $\alpha = \beta = 1$. Putting all this together into Eq. (A1), we obtain Eq. (3). The integral expression, $Y(\Omega)$ has the property that it is purely real for $\Omega < 0$. It may be written in the useful alternative form

$$Y(\Omega) = \Omega^{1/2}\exp(-\Omega)\left(-i\pi^{1/2} + \int_0^\Omega dz\, z^{-1/2}\exp z\right).$$

[1] S. Ejima and Doublet III Group, Nucl. Fusion **22**, 1627 (1982).
[2] F. L. Hinton and R. D. Hazeltine, Rev. Mod. Phys. **48**, 240 (1976).
[3] C. S. Chang and F. L. Hinton, Phys. Fluids **25**, 1493 (1982); **29**, 3314 (1986).
[4] M. Greenwald, D. Gwinn, S. Milora, J. Parker, R. Parker, and S. Wolfe, in *Plasma Physics and Controlled Nuclear Fusion Research, 1984,* Proceedings of the 10th International Conference, London (IAEA, Vienna, 1985), Vol. I, p. 45; S. Wolfe and M. Greenwald, Nucl. Fusion **26**, 329 (1986).
[5] H. Niedermeyer and ASDEX Team, in *Plasma Physics and Controlled Nuclear Fusion Research, 1986,* Proceedings of the 11th International Conference, Kyoto (IAEA, Vienna, 1987), Vol. I, p. 125.
[6] R. J. Groebner, W. W. Pfeiffer, F. P. Blau, K. H. Burrell, E. S. Fairbanks, R. P. Seraydarian, H. St. John, and R. E. Stockdale, Nucl. Fusion **26**, 543 (1986).
[7] R. Hawryluck and TFTR Group, in Ref. 5, Vol. I, p. 51.
[8] V. Mertens, W. Sandmann, M. Kaufmann, R. S. Lang, K. Büchl, H. Murmann, ASDEX Team, and NI Team, in *Proceedings of the 15th European Conference on Controlled Fusion and Plasma Heating,* Dubrovnik (European Physical Society, Budapest, 1988), Vol. I, p. 39.
[9] D. L. Brower, W. A. Peebles, S. K. Kim, N. C. Luhmann, Jr., W. M. Tang, and P. E. Phillips, Phys. Rev. Lett. **59**, 49 (1987).
[10] O. Gehre, O. Gruber, H. D. Murmann, D. E. Roberts, F. Wagner, B. Bomba, A. Eberhagen, H. U. Fahrbach, G. Fussmann, J. Gernhardt, K. Hübner, G. Janeschitz, K. Lackner, E. R. Müller, H. Niedermeyer, H. Röhr, G. Staudenmaier, K. H. Steuer, and O. Vollmer, Phys. Rev. Lett. **60**, 1502 (1988).
[11] L. I. Rudakov and R. Z. Sagdeev, Dokl. Akad. Nauk SSSR **138**, 581 (1961) [Sov. Phys. Dokl. **6**, 415 (1965)].
[12] O. P. Pogutse, Sov. Phys. JETP **25**, 498 (1968).
[13] B. Coppi, M. N. Rosenbluth, and R. Z. Sagdeev, Phys. Fluids **10**, 582 (1967).
[14] G. S. Lee and P. H. Diamond, Phys. Fluids **29**, 3291 (1986).
[15] P. W. Terry, J. N. Leboeuf, P. H. Diamond, D. R. Thayer, J. E. Sedlak, and G. S. Lee, Phys. Fluids **31**, 2920 (1988).
[16] W. Horton, D- I. Choi, and W. M. Tang, Phys. Fluids **24**, 1077 (1981).
[17] P. N. Guzdar, L. Chen, W. M. Tang, and P. H. Rutherford, Phys. Fluids **26**, 673 (1983).
[18] B. B. Kadomtsev and O. P. Pogutse, Nucl. Fusion **11**, 67 (1971).
[19] M. Tagger, G. Laval, and R. Pellat, Nucl. Fusion **17**, 109 (1977).
[20] W. M. Tang, J. C. Adam, and D. W. Ross, Phys. Fluids **20**, 430 (1977).
[21] H. Biglari, P. H. Diamond, and P. W. Terry, Phys. Rev. Lett. **60**, 200 (1988).
[22] H. Biglari, P. H. Diamond, and P. W. Terry, Phys. Fluids **31**, 2644 (1988).
[23] JET Team, in Ref. 5, Vol. I, p. 31.
[24] J. P. Christiansen, J. D. Callen, J. G. Cordey, and K. Thomsen, submitted to Nucl. Fusion (1988).
[25] F. Wagner and ASDEX team, Phys. Rev. Lett. **49**, 1408 (1982).
[26] K. McGuire and PDX Group, in Ref. 4, Vol. I, p. 117.
[27] K. H. Burrell and DIII-D Group, Phys. Rev. Lett. **59**, 1432 (1987).
[28] W. M. Tang, G. Rewoldt, and L. Chen, Phys. Fluids **29**, 3715 (1987).
[29] R. R. Dominguez and R. E. Waltz, Phys. Fluids **31**, 3147 (1988).
[30] R. R. Dominguez and R. E. Waltz, Nucl. Fusion **27**, 96 (1987).
[31] J. W. Connor, R. J. Hastie, and J. B. Taylor, Phys. Rev. Lett. **40**, 396 (1978); A. Glasser, Y. C. Lee, and J. W. Van Dam, in *Proceedings of the Finite Beta Theory Workshop,* edited by B. Coppi and W. Sadowski (U.S. Department of Energy, Washington, DC, 1977), pp. 55 and 93.
[32] M. N. Rosenbluth, D. W. Ross, and D. P. Kostamorov, Nucl. Fusion **12**, 3 (1971).
[33] R. J. Goldston, Y. Takase, D. C. McCune, M. G. Bell, M. Bitter, C. E. Bush, P. H. Diamond, P. C. Efthimion, E. D. Frederickson, B. Grek, H. Hendel, K. W. Hill, D. W. Johnson, D. Mansfield, K. McGuire, E. Nieschmidt, H. Park, M. H. Redi, J. Schivell, S. Sesnic, and G. Taylor, in *Proceedings of the Fourteenth European Conference on Controlled Fusion and Plasma Physics,* edited by S. Methfessel (European Physical Society, Budapest, 1987), Vol. I, p. 140.
[34] L. Chen, R. W. White, and M. N. Rosenbluth, Phys. Rev. Lett. **52**, 1122 (1984).
[35] J. Wieland and L. Chen, Phys. Fluids **28**, 1359 (1985).
[36] H. Biglari and L. Chen, Phys. Fluids **29**, 2960 (1986).
[37] H. Biglari and P. H. Diamond, Phys. Fluids **30**, 3735 (1987).
[38] B. Coppi and G. Rewoldt, Phys. Rev. Lett. **33**, 1329 (1974); B. Coppi and F. Pegoraro, Nucl. Fusion **17**, 969 (1977).
[39] R. E. Waltz, submitted to Phys. Fluids.